SAND97-3167C
SAND--97-3167C
CONF-980605--

Axial Diagnostic Package for Z

T. J. Nash, M. S. Derzon, G. Chandler, D. Fehl, R. Leeper, M. Hurst, D. Jobe, J. Torres, J. Seaman, S. Lazier, T. Gilliland and J. McGurn
Sandia National Laboratories, Albuquerque, NM, 87185-1193

RECEIVED
JUN 08 1998
OSTI

ABSTRACT

We have developed and fielded an axial diagnostic package for the 20 MA, 100 ns, z-pinch driver Z. The package is used to diagnose dynamic hohlraum experiments which require an axial line of sight. The heart of the package is a reentrant cone originally used to diagnose ion-beam-driven hohlraums on PBFA-II. It has one diagnostic line of sight at 0 degrees, 4 at 6 degrees, and 4 at 9 degrees. In addition it has a number of viewing, alignment, and vacuum feedthrough ports. The front of the package sits approximately 5 feet from the pinch. This allows much closer proximity to the pinch, with inherently better resolution and signal, than is presently possible in viewing the pinch from the side. Debris that is preferentially directed along the axis is mitigated by two apertures for each line of sight, and by fast valves and imaging pinholes or cross slits for each diagnostic. In the initial run with this package we fielded a time resolved pinhole camera, a five-channel pinhole-apertured x-ray diode array, a bolometer, a spatially resolved time-integrated crystal spectrometer, and a spatially and temporally resolved crystal spectrometer. We will present data obtained from these diagnostics in the dynamic hohlraum research conducted on Z.

Sandia is a multiprogram laboratory operated by Sandia Corporation, a Lockheed Martin Company, for the United States Department of Energy under contract DE-AC04-94AL85000.

I. Introduction

We have developed an axial package for diagnosing dynamic hohlraum experiments on Z, a 20 MA, 100 ns driver. (1) The concept of the dynamic hohlraum is that a z-pinch itself acts as an imploding radiation case. (2,3,4). Radiation is produced via a strongly radiating shock wave when an outer z-pinch liner or shell strikes an inner liner. The collision produces radiation which is trapped inside if the outer liner is optically thick. The ongoing implosion after the collision of the liners compresses the trapped radiation to higher temperatures. This radiation could then be used to ablate and drive a fusion capsule. (5) To diagnose the radiation temperatures in such an imploding hohlraum it is necessary to view the pinch along the axis, since views from the side are obscured by the opacity of the pinch.

We have refurbished an axial reentrant cone originally designed to diagnose ion beam driven hohlraums on the machine PBFA-II. The reentrant cone was adapted to Z with a hemispherical lid that positions the cone at the proper distance from the pinch. This package is conceptually depicted in figure 1. After a shot the reentrant cone is hoisted from the axis and parked in a docking bay, because axial access is necessary for turning the machine Z around for the next shot. The cabling to the various diagnostics is long enough that it may remain connected while moving the axial package from machine center to the nearby docking port.

Debris is a severe problem along the axis of a pinch on Z which radiates up to 2 MJ and sends shrapnel flying on ballistic trajectories along the axis. Because of this debris problem each line of sight is protected by two apertures. At 20 inches from the pinch a copper plate 1/4" thick with 1 inch diameter apertures for each line of sight provides the first line of debris protection for the package. At the front of the reentrant cone approximately 60 inches from the pinch a second aperture customized to the diagnostic in use, typically a circle or slot aperture, provides a second line of debris protection. Finally all diagnostics are protected along their individual beamlines by either fast valves or imaging apertures or both.

The package uses three universal manifolds for operating diagnostic vacuums and fast valves, one for roughing vacuum, one for turbomolecular pump forelines, and one for high pressure nitrogen to drive fast valves. In this way several diagnostics can share the same vacuum hardware.

We will present results from several axial diagnostics. These include a filtered x-ray diode array, a bolometer, a time-resolved pinhole camera, and crystal spectrometers.

II. Axial Package Diagnostics

For initial dynamic hohlraum experiments on Z the axial diagnostics consisted of a filtered x-ray diode array, a bolometer, time-resolved pinhole cameras, and crystal spectrometers. The package is of course amenable to other diagnostics as well. For instance streaked grazing incidence spectrometers and streaked filtered scintillators have also been fielded.

The five-channel x-ray diode set is filtered with 4µm kimfol, 1µm vanadium, .75µm zinc with 1 µm parylene, 8 µm beryllium with 1 µ parylene, and 9 µm beryllium with 1 µm parylene. The nominal bandpasses of the above filters are at 250, 450, 650, 850, and 1400 eV. The x-ray diodes were absolutely calibrated at the National Synchrotron facility at Brookhaven National Laboratory.

The bolometer element is nickel 1 mm wide and 9 mm long. It is apertured to a 3 mm length to reduce signal. The nickel element is 1 µm thick. The time response of the bolometer is 1 to 2 ns, not fast enough to actually measure peak power. We use the bolometer to measure x-ray yield, and estimate radiated power by normalizing the kimfol-filtered x-ray diode signal integral to the yield from the bolometer. The power may also be estimated by fitting a Planckian to the signals from the 5 x-ray diode channels.

The time-resolved pinhole cameras use microchannel plates coated with twelve half-strips of gold to conduct gating pulses. We drive the strips with gates less than 1 ns and separate adjacent strips by 1 ns. We gate 11 strips, recording 11 pinch images over an 11 ns duration. The twelfth strip is time-integrated. We presently record data with two such instruments. Two pinhole images are recorded on each half-strip, one is filtered with 5 μm of kimfol for a bandpass at 250 eV, the other is filtered with 8 μm of beryllium and 1 μm of parylene for a bandpass above 800 eV. The magnification of the cameras is 2/3. The pinholes are 100 μm diameter, giving 250 μm pinhole limited resolution at the pinch.

We field a radially resolved time-integrated crystal spectrometer. Is uses a 300 μm cross slit with magnification of 1 for 600 μm spatial resolution in the pinch radius. It uses a KAP crystal with a 25 μm beryllium filter. We also field a seven-frame time-resolved crystal spectrometer. This instrument is under development for measuring K lines of tracer elements such as sodium and fluorine and taking line ratios as one technique to record dynamic hohlraum temperature. It will also be used to do tracer spectroscopy of pellet implosions looking at the K lines of elements such as sulfur and argon.

III. Results from Axial Package Diagnostics

We will present a summary of results obtained with the axial package on Z shot 214. The pinch load for this shot is depicted in figure 2. It is a plastic foil within a nested tungsten wire array. The outer part of the nest is 240 7.5μm tungsten wires at a 2 cm radius weighing 2 mg . The inner part of the nest is 120 7.5 μm tungsten wires at a 1 cm radius weighing 1 mg. The plastic annulus is at a 5 mm diameter and weighs 2.5 mg. The pinch is 1 cm long. At the bottom of the plastic annulus, on the cathode side of the pinch, is a gold half-moon to serve as a fiducial, and verify that the inside of the dynamic hohlraum is optically thin. Experiments in which a fusion pellet is placed inside of the plastic annulus will take place late in 1998 on Z.

The power radiated out the end of the pinch through a 5.8 mm aperture is shown in figure 3. This curve is obtained by using the bolometer to normalize the kimfol-filtered x-ray diode signal. Also shown is the power radiated out the side of the pinch. This curve is recorded with similar diagnostics fielded on the side of the pinch. The two curves have drastically different time dependence due to the effects of opacity of the pinch. The axial power rises more rapidly than the side power because radiation is trapped inside the pinch during the implosion. The burst in the x-ray power out the side occurs when the pinch wall is heated enough that the liner goes thin, allowing radiation to escape. We have found that using a solid current return can, and thereby blocking off the side-on diagnostics, improves the dynamic hohlraum temperature by 15%. Figure 3 also depicts the timing of gates 4 through 11 for one of the time-resolved pinhole cameras. The gates are well timed to record dynamic hohlraum images during the rise of the axial x-ray power when the dynamic hohlraum temperature is increasing.

Figure 4 shows the kimfol-filtered image of gate number 8 on this shot. At the time of this gate the axial x-ray power is about 5 TW. This power is used to normalize the image in figure 4, and provide the two-dimensional spatial profile of the dynamic hohlraum radiation temperature. In figure 4 the gold half-moon is clearly evident, showing that the inside of the hohlraum is thin over the 1 cm length of the pinch. The image is distorted from circular because the line of sight is at a 6 degree angle with the axis.

By taking line-outs perpendicular to the gold and plastic half-moons interface one obtains the temperature profile of the dynamic hohlraum shown in figure 5. The dynamic hohlraum heats at a rate of about 20 eV/ns as the pinch implodes. With the time-resolved pinhole camera several regions of the dynamic hohlraum are detected: the tungsten wall, the gold half-moon, the plastic half-moon, and the plastic wall of the annular target. The temperatures of these regions are plotted in figure 6. In the initial time frame at 527 ns, the plastic half-moon and plastic wall are in equilibrium. At 529 ns the plastic wall burns through, becomes optically thin, and is no longer detected. As the plastic wall burns through the gold half moon and tungsten wall come into equilibrium. At 530 ns the gold half-moon begins to lag the tungsten wall in temperature. This is thought to be due to absorption by tungsten that blows over the plastic target and obscures the view of the gold half-moon. The true dynamic hohlraum temperature would be represented by at least the temperature of the tungsten wall. Since the hohlraum is still open at 532 ns with a 180 eV wall temperature, we extrapolate that this dynamic hohlraum reached a temperature of 190 eV. We expect that this temperature will increase when the identical load is shot with a solid current-return can.

IV. Summary

We have modified a reentrant diagnostic cone originally developed for ion beam driven hohlraum experiments to serve as a frame for axial diagnostics for dynamic hohlraum z-pinch experiments on the driver Z. The package is well apertured to protect against the severe debris ejected along the axis of a pinch. The package is removed from the machine axis between shots to allow for machine turnaround , and is parked in a nearby docking bay. The package has nine ports, one on axis, four at 6 degrees, and four at 9 degrees. We have used the package to diagnose dynamic hohlraum experiments on Z. We field an x-ray diode array, a bolometer, two time-resolved pinhole cameras , and crystal spectrometers. We use the bolometer and the x-ray diodes to measure power radiated out the axis. We then use the time-resolved x-ray images to unfold the spatial profile of the dynamic hohlraum temperatures. A temperature of 180 eV has been measured while the dynamic hohlraum is still open.

References

1. R. B. Spielman, C. Deeney, G. A. Chandler, M. R. Douglas, D. L. Fehl, M. K. Matzen, D. H. McDaniel, T. J. Nash, J. L. Porter, T. W. L. Sanford, J. F. Seamen, W. A. Stygar, K. W. Struve, S. P. Breeze, J. S. McGurn,

J. A. Torres, D. M. Zagar, T. L. Gilliland, D. O. Jobe, J. L. McKenney, R. C. Mock, M. Vargas, T. Wagoner, and D. L. Peterson, Proc. of the 11th Int. Conf. on Particle Beams, edited by K. Jungwirth and J. Ullschmied, Prague, Czech Republic, 1996, p. 150

2. R. Bowers and J. Brownell, "The Flying Radiation Case," Bull. of the 37th meeting of the APS-DPP, November, 1995, NIST# DE-97004733

3. V. P. Smirnov, Plasma Physics and Controlled Fusion, **33**, #13, 1697, (1991)

4. T.J. Nash, M.S. Derzon, G. Allshouse, C. Deeney, J.F. Seaman, J. McGurn, D. Jobe, T. Gilliland, J.J. MacFarlane, P. Wang, and D.L. Petersen , "Dynamic Hohlraum Experiments on SATURN," Proceedings of the 4th International Conference on High-Density Z-pinches, Vancouver, Canada, p. 175, May, 1997

5. J. Lendl, Phys. Plasmas, **2** (11), November 1995

Figure Captions

1. The axial reentrant cone with attached diagnostics and its insertion into the adapting hemispherical lid and its view of the z-pinch is depicted.

2. An axial schematic view of a dynamic hohlraum z-pinch load. A nested tungsten wire array implodes onto a plastic annulus. A gold half-moon serves as an x-ray fiducial from the back wall of the hohlraum.

3. Power radiated out the end and side of Z shot 214 as a function of time. Gates 4 through 11 of the axial time-resolved pinhole camera are depicted.

4. Gate 8 time-resolved pinhole image at the 250 eV bandpass. The gold half -moon is clearly evident.

5. Radial temperature dependence of the dynamic hohlraum of Z shot 214 parametric in time. This profiles recorded with the time-resolved pinhole camera using the x-ray diodes and bolometer for normalization. The tungsten wall heats to 180 eV while the hohlraum is still open.

6. The time-resolved pinhole camera records temperatures of several regions of the dynamic hohlraum. As the plastic wall of the target burns through the gold half-moon equilibrates with the tungsten wall. The apparent gold temperature later lags the wall temperature due to absorption by tungsten blowing over the target and closing off the end of the hohlraum .

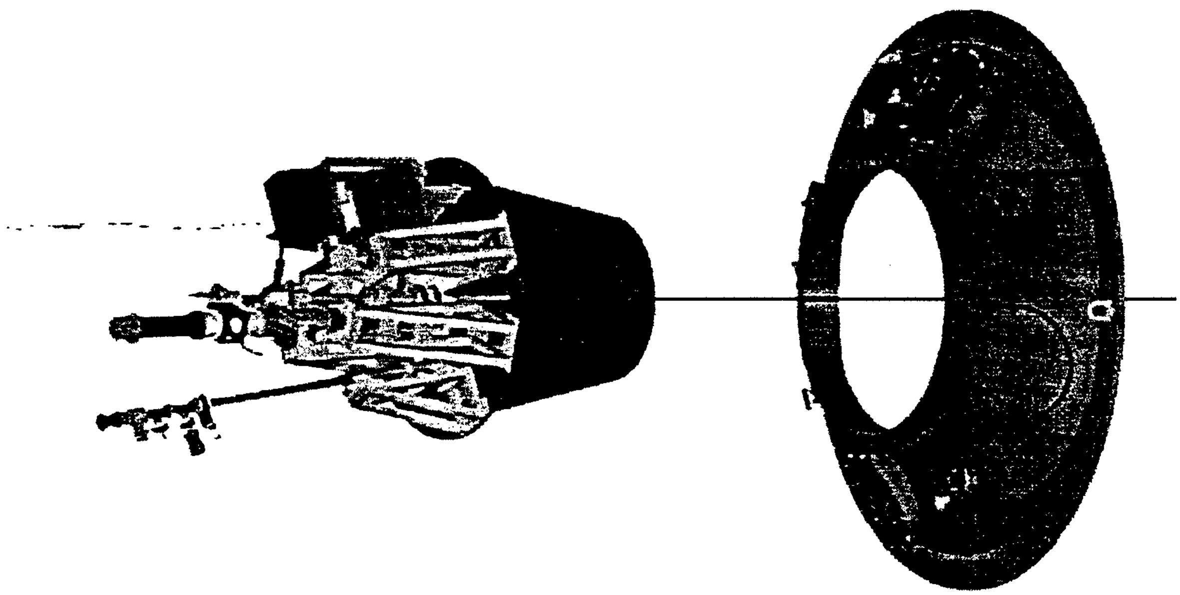

240/120 W 7.5 µm wires
2/1 cm radii
2/1 mg mass
1 cm long

2.5 mg plastic annular
target at 2.5 mm radius

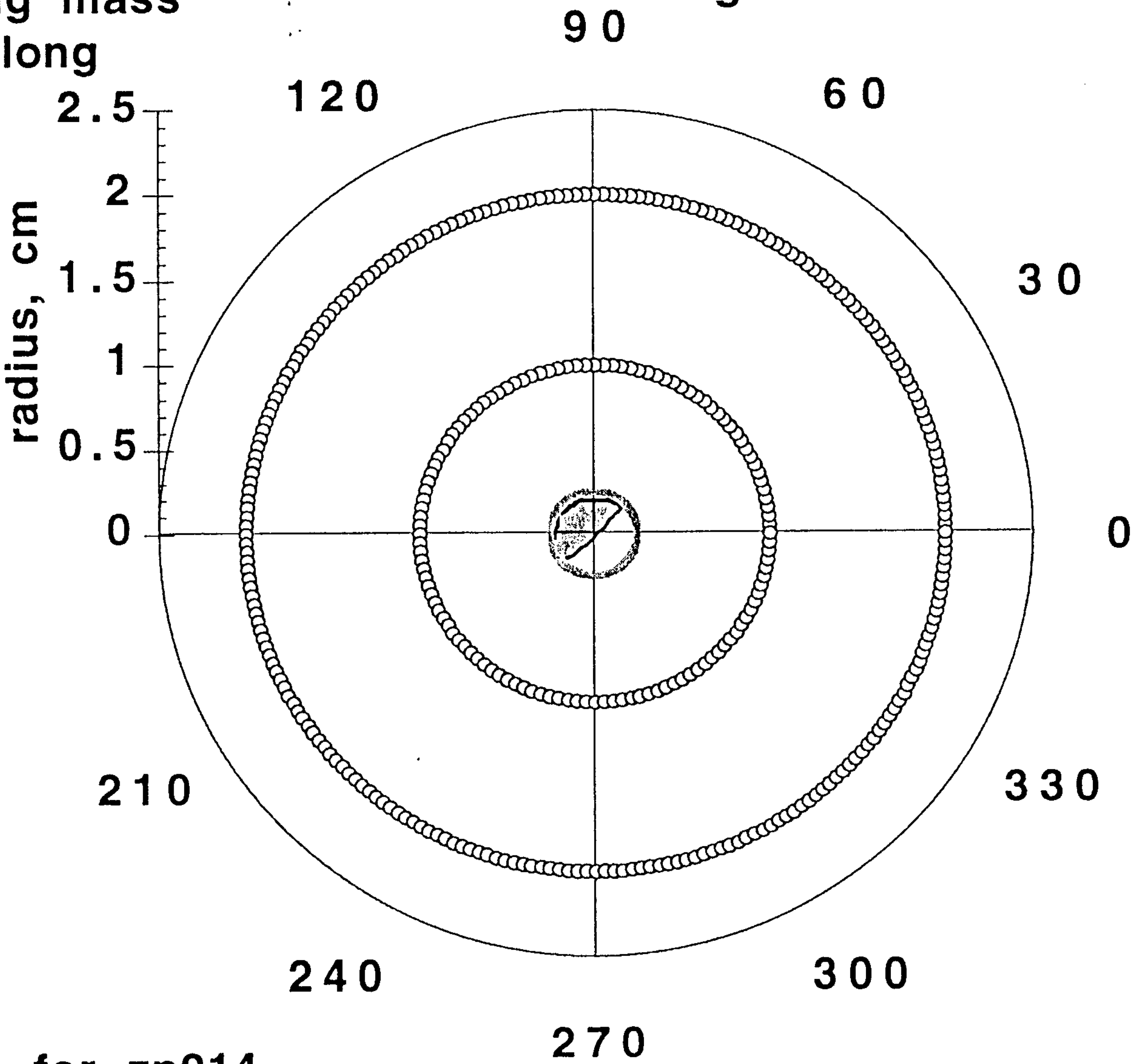

load for zp214

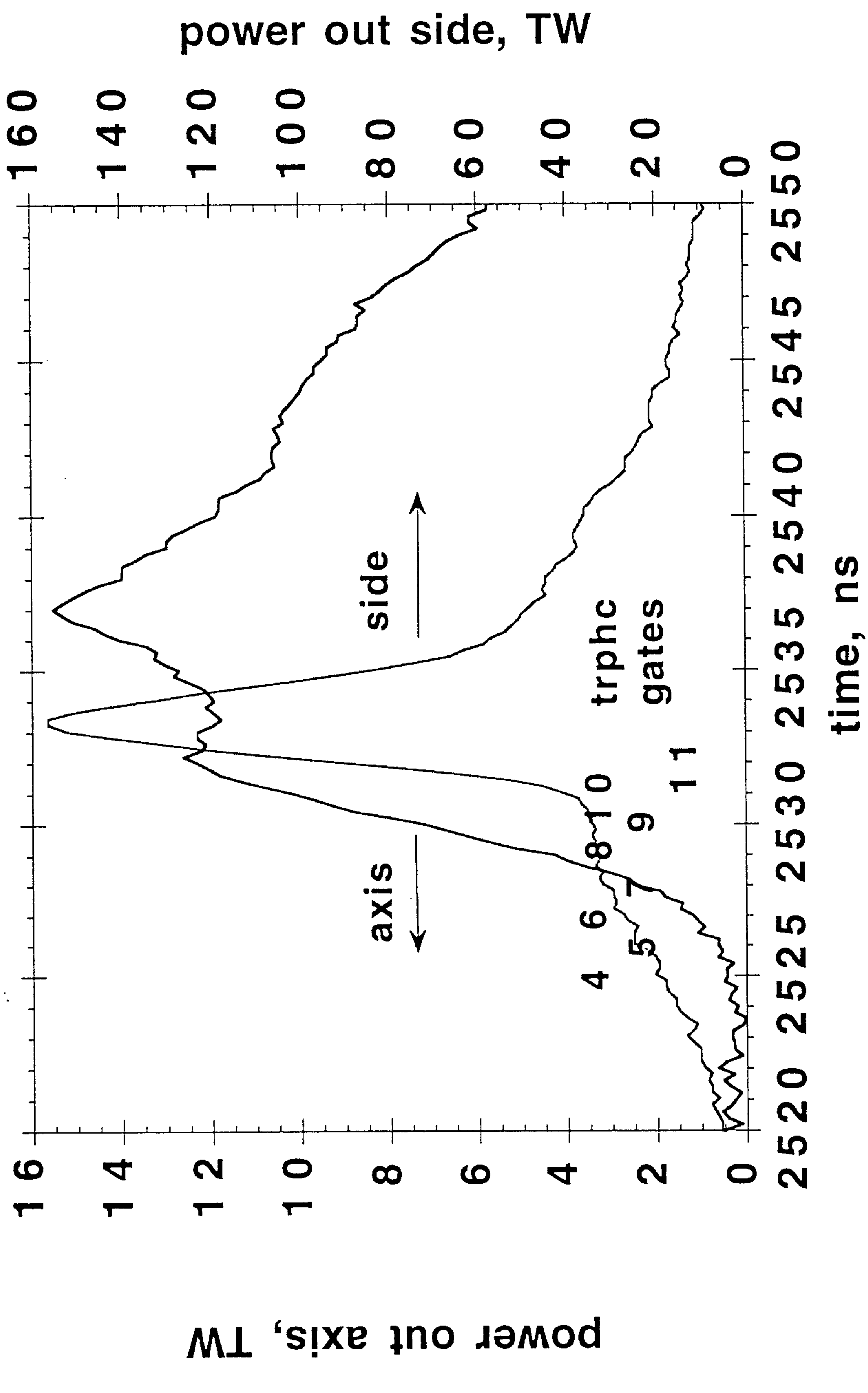
power out side, TW
power out axis, TW
time, ns
side
axis
trphc gates
4
5
6
7
8
9
10
11
0
20
40
60
80
100
120
140
160
0
2
4
6
8
10
12
14
16
2520
2525
2530
2535
2540
2545
2550

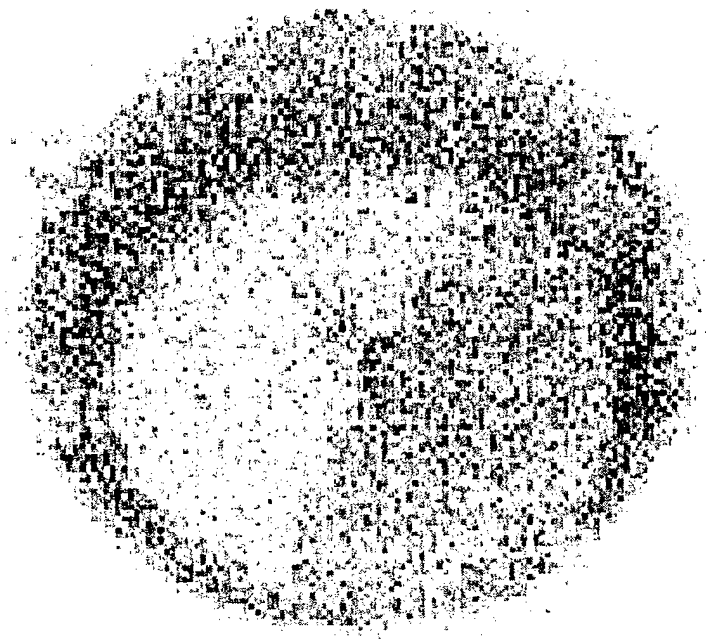

zp 214
1 ns gate
hohlraum
image
5 ns
before
closure

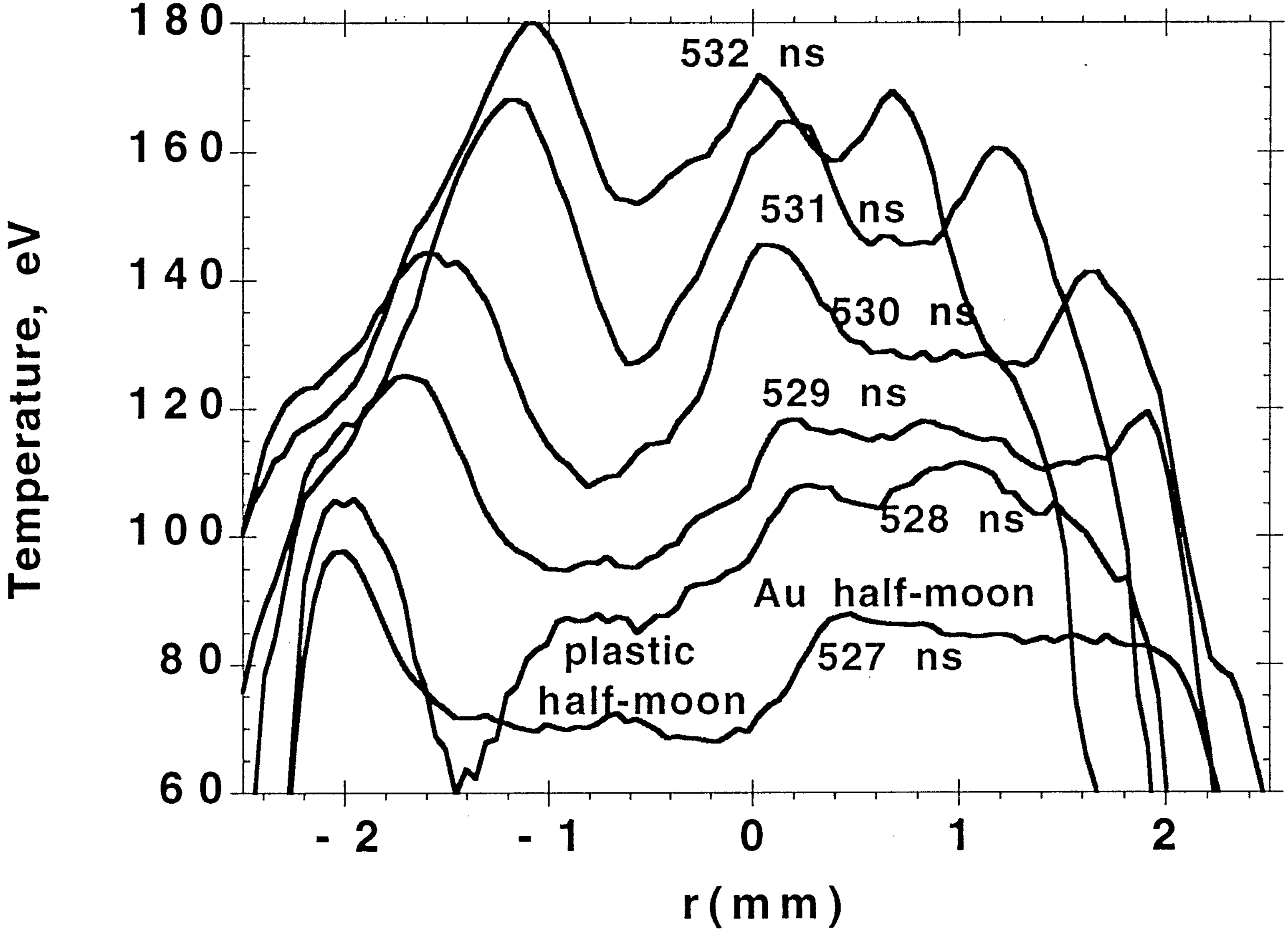
180
160
140
120
100
80
60
Temperature, eV
532 ns
531 ns
530 ns
529 ns
528 ns
527 ns
Au half-moon
plastic
half-moon
- 2
- 1
0
1
2
r (mm)

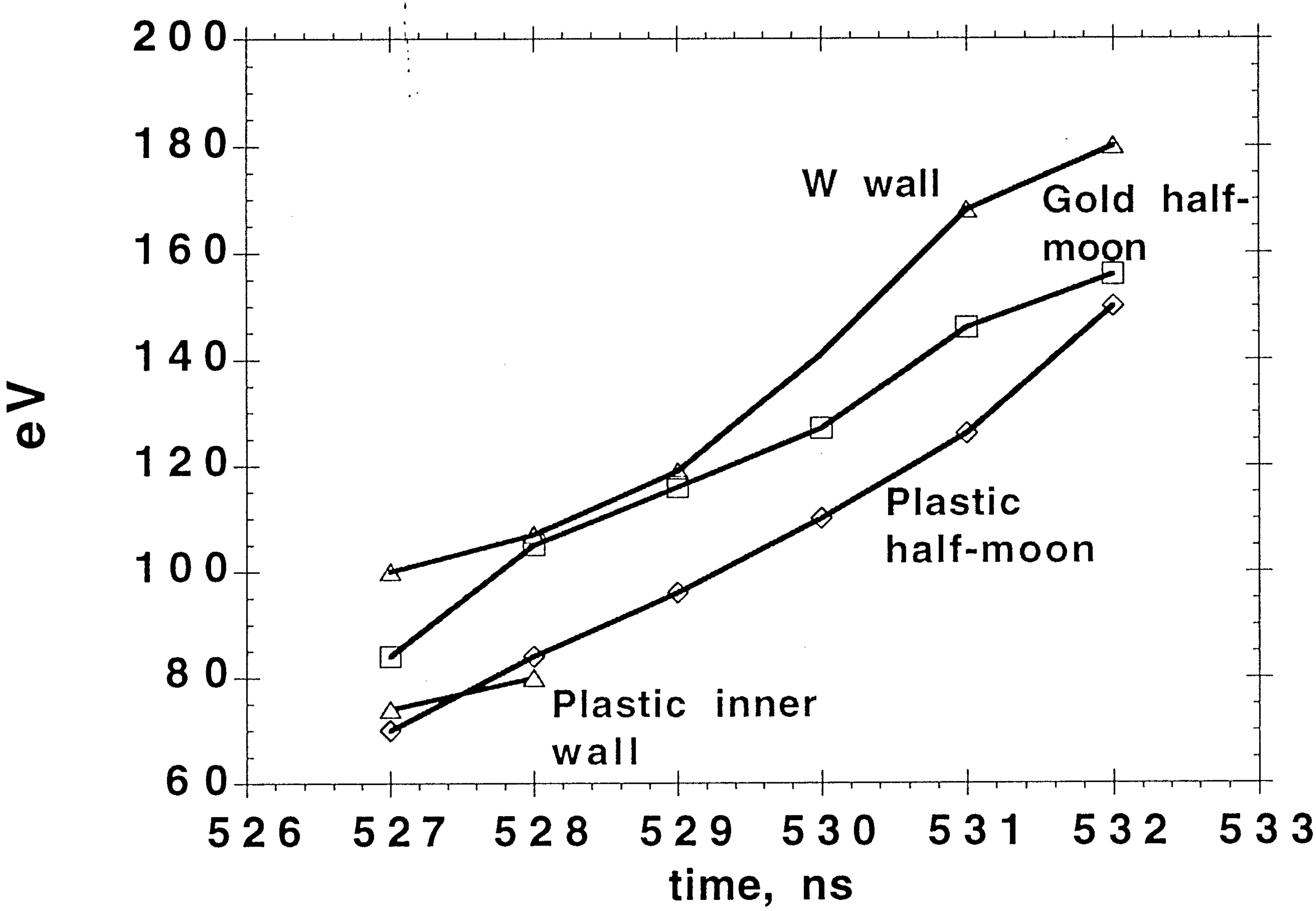

eV
200
180
160
140
120
100
80
60
526
527
528
529
530
531
532
533
time, ns
W wall
Gold half-moon
Plastic half-moon
Plastic inner wall

Report Number (14) SAND--97-3167C

CONF-980605--

Publ. Date (11) 199806

Sponsor Code (18) DOE/DP, XF

UC Category (19) UC-700, DOE/ER